

## Transition probabilities in OH A2Σ+–X2Πi: Bands with v' = 2 and 3

Kristen L. Steffens, Jorge Luque, Jay B. Jeffries, and David R. Crosley

Citation: *J. Chem. Phys.* **106**, 6262 (1997); doi: 10.1063/1.473644

View online: <http://dx.doi.org/10.1063/1.473644>

View Table of Contents: <http://jcp.aip.org/resource/1/JCPSA6/v106/i15>

Published by the AIP Publishing LLC.

---

### Additional information on J. Chem. Phys.

Journal Homepage: <http://jcp.aip.org/>

Journal Information: [http://jcp.aip.org/about/about\\_the\\_journal](http://jcp.aip.org/about/about_the_journal)

Top downloads: [http://jcp.aip.org/features/most\\_downloaded](http://jcp.aip.org/features/most_downloaded)

Information for Authors: <http://jcp.aip.org/authors>

## ADVERTISEMENT



**RUN YOUR GPU  
CODE 2X FASTER.  
TRY A TESLA K20 GPU  
ACCELERATOR TODAY.  
FREE.**

# Transition probabilities in OH $A^2\Sigma^+ - X^2\Pi_i$ : Bands with $v' = 2$ and 3

Kristen L. Steffens,<sup>a)</sup> Jorge Luque, Jay B. Jeffries, and David R. Crosley  
Molecular Physics Laboratory, SRI International, Menlo Park, California 94025

(Received 25 November 1996; accepted 10 January 1997)

Experimental relative vibrational band emission coefficients have been measured in the  $A^2\Sigma^+ - X^2\Pi_i$  electronic system of the OH radical. Branching ratios for the sequences  $v' = 2$ ,  $v'' = 0-5$  and  $v' = 3$ ,  $v'' = 0-6$  were determined using laser-induced fluorescence in a low pressure methane-oxygen flame. We accounted for potential error contributed by rotational and vibrational energy transfer and fluorescence polarization. These transition probabilities complete a set of experimental data, which are used in a separate study to determine the optimum electronic transition moment of the OH  $A-X$  system. © 1997 American Institute of Physics. [S0021-9606(97)00315-2]

## I. INTRODUCTION

The OH radical is an important reaction intermediate in many chemical processes, including combustion<sup>1</sup> and atmospheric chemistry,<sup>2</sup> and has been the subject of many molecular dynamics studies.<sup>3</sup> In addition, the OH radical has few enough electrons to be a good candidate for accurate theoretical calculations,<sup>4</sup> and it is easy to detect using the technique of laser-induced fluorescence (LIF). Hence, the spectroscopic properties of OH are of great interest in many contexts and are often possible to determine both experimentally and theoretically.

For many experiments involving OH, relative or absolute rotational- and vibrational-state-specific transition probabilities within the  $A^2\Sigma^+ - X^2\Pi_i$  system must be known. In a large number of cases, the diagonal transitions with  $\Delta v = 0$  are utilized; these have been extensively studied previously. Recently, there has been increased interest in the use of the weaker, off-diagonal bands. This includes the measurement of OH concentrations in combustion environments by excitation of the  $v' = 3$  level,<sup>5</sup> and quantification of the interference in tropospheric OH measurements caused by ozone photolysis.<sup>6</sup> Additionally, the off-diagonal bands are good candidates to probe vibrational energy transfer<sup>7</sup> (VET) and rotational energy transfer<sup>8</sup> (RET) in the ground state, and to characterize product state distributions in chemical reactions.<sup>4</sup> For these generally weaker bands the state-specific transition probabilities are not so well characterized.

Early experimental transition probability studies on the stronger bands were primarily done via emission<sup>9</sup> or absorption<sup>10</sup> intensities. More recent determinations were done using the LIF technique, including earlier studies by Crosley and Lengel<sup>11</sup> (CL) on  $v' = 0, 1$ , and 2, by Copeland *et al.*<sup>12</sup> on  $v' = 0$  and 1, and by Andresen *et al.*<sup>5</sup> (AM) on the highly predissociated  $v' = 3$  level.

Accurate and consistent sets of experimental vibrational band transition probabilities  $p_{v',v''}$  ratios form the basis of calculated sets of rotational/vibrational transition probabilities. Calculated rotational-level-specific transition probabilities are extremely important, because they are difficult to

determine accurately by direct measurement, but are used extensively in such applications as LIF temperature determinations. Because the  $A-X$  transition moment  $R_e(r)$  varies sharply with internuclear distance  $r$ , an accurate  $R_e(r)$  is needed for this purpose. Early empirical forms<sup>11</sup> of  $R_e(r)$  were determined from experimental  $p_{v',v''}$ . An excellent form of  $R_e(r)$  is that produced by recent theoretical calculations.<sup>4</sup> This study predicts an  $R_e(r)$  that linearly decreases with  $r$  at short internuclear distance, in agreement with the empirical forms, but dropping to a negative minimum at about 1.7 Å and returning asymptotically to zero at large  $r$ . This moment, together with accurate Rydberg-Klein-Rees (RKR) rovibrational wave functions, can be used to calculate a comprehensive set of rotational/vibrational specific transition probabilities. However, accurate values for the weaker, off-diagonal bands, such as (3,0), require experimental data for those bands to test the theoretical fits of  $R_e(r)$  at small and large internuclear distance.

In this study,  $p_{v',v''}$  from the slightly predissociated  $v' = 2$  level to  $v'' = 0-5$  and from the highly predissociated level  $v' = 3$  to  $v'' = 0-6$  are measured, using LIF, to improve the accuracy with which these values are known. These measurements, together with those of Copeland *et al.*<sup>12</sup> serve as valuable input to a new set of transition probability calculations<sup>13</sup> spanning a wide range of  $v$  and  $J$ .

## II. EXPERIMENT

The experiments were conducted in a low-pressure combustion chamber having optical access, within the burnt gases of a premixed, roughly stoichiometric  $\text{CH}_4\text{-O}_2$  flame operated at pressures in the range 7–14 Torr. In this region there exist copious quantities of OH, on the order of  $5 \times 10^{14} \text{ cm}^{-3}$ . Vertically polarized, unfocused laser light near 245, 269, or 262 nm excited the (3,0), (3,1), or (2,0) bands, respectively; these wavelengths were generated by frequency doubling the output of a 355 nm (tripled YAG) pumped dye laser. A UG5 spectral filter separated out residual visible laser light to minimize scattered light complications. The fluorescence emitted by the excited OH was collected and collimated by a lens at a right angle to the laser beam, and

<sup>a)</sup>Currently at the National Institute of Standards and Technology, Gaithersburg, Maryland 20899.

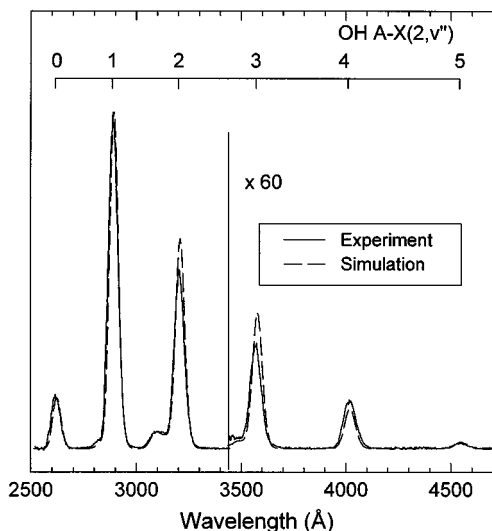


FIG. 1. Low resolution (40 Å FWHM) fluorescence spectrum of OH (A-X) ( $2,v''$ ) after pumping  $Q_1(4)$  (2,0) in a  $\text{CH}_4\text{-O}_2$  flame at 7 Torr total pressure. The simulated spectrum is shown in dashed line.

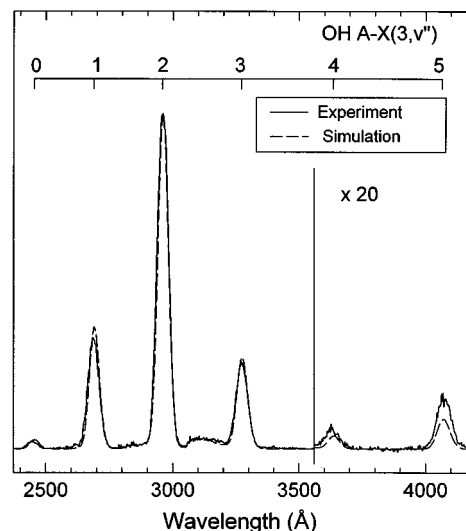


FIG. 2. Low resolution (40 Å FWHM) fluorescence spectrum of OH (A-X) ( $3,v''$ ) in a 14 Torr  $\text{CH}_4\text{-O}_2$  flame. The simulated spectrum is shown in dashed line.

focused onto the front slit of a 0.35 m focal length spectrometer of resolution 2 nm/mm equipped with 250 and 500 nm blazed gratings. Typical resolution was 3 to 4 nm for “low resolution” dispersed fluorescence scans and 0.8 nm for “high-resolution” scans. The fluorescence was detected with an EMI 9558Q photomultiplier, amplified one hundredfold, and fed into a boxcar integrator with 10 ns gate width. This short gate is used to discriminate against complications caused by VET even at this low pressure; little signal level is sacrificed because the overall lifetimes of  $v'=2$  and 3 are short. The spectral response of the entire system was calibrated using standard Optronics lamps; tungsten in the visible and deuterium in the ultraviolet. The total fluorescence was continually measured using a filtered Hamamatsu photomultiplier to monitor fluctuations in laser power or OH concentration.

In each vibrational band,  $Q_1(4)$  was chosen as the excitation line for several reasons. It is strong, and  $N''=4$  is one of the most highly populated rotational levels at flame temperatures, ensuring a high signal to noise ratio. For the same reason, exciting  $N'=4$  helps minimize the influence of rotational redistribution in the  $A^2\Sigma^+$  state. Moreover, in many bands with  $v'=2$  and 3, there is little rotational dependence of vibrational band ratios (see Refs. 4 and 13) for low  $N$ . Thus any RET into neighboring levels will produce small changes in relative  $p_{v',v''}$  compared to ratios obtained had no RET occurred.

The relative intensities of the ( $2,v''$ ) sequence were determined by exciting in the (2,0) band and dispersing the resulting fluorescence. These bands occur over a wide wavelength range (250–480 nm). Thus 4 nm resolution scans were taken using the 500 nm grating for the (2,1) through (2,5) bands, and 3 nm resolution scans with the 250 nm grating for (2,0) through (2,2). The (2,1) and (2,2) bands are used to splice together the two sets, which are shown in Fig. 1. Scans over the (2,3) to (2,5) bands were made at increased

laser power to observe the weak (2,5) band; the (2,3) and (2,4) intensities were used to scale these results to the other bands. Laser scatter in the (2,0) region was subtracted, using a scan with the laser tuned slightly off resonance. The contribution of laser scatter to the total apparent (2,0) intensity in Fig. 1 is about 5%.

The  $v'=3$  bands were measured in the same way, exciting in (3,0). The 500 nm blazed grating was used to collect the (3,0) through (3,5) bands, shown in Fig. 2. Only an upper limit for (3,6) could be determined. The (3,0) band is about eight times weaker than (2,0), so that higher laser intensity is needed for excitation, and scatter poses a larger problem, contributing about 80% of the apparent (3,0) band intensity. To obtain a more reliable value for (3,0), we excited the (3,1) band and scanned over the (3,0) and (3,2) bands, using the 250 nm grating with a resolution of 3.6 nm.

In both Figs. 1 and 2, emission from lower lying vibrational levels can be seen. This occurs due to a small amount of VET occurring from these levels in the flame,<sup>14</sup> despite the low pressure and short, prompt gate. Their contributions to the apparent intensities of the bands having  $v'=2$  and 3 must be accounted for. This was done using spectral simulations, described in the following section. The rotational population distribution in the excited vibrational levels is required for this purpose, so scans of the more intense bands were performed at high resolution. These are shown in Fig. 3 and 4.

### III. ANALYSIS AND RESULTS

#### A. Spectral simulations

The transition probability for each band is proportional to the area under the peak. However, some bands, especially (2,1), (2,2), (3,2), and (3,3) are complicated by VET to lower vibrational levels, which emit strong bands in the same wavelength region. The VET contribution to the observed

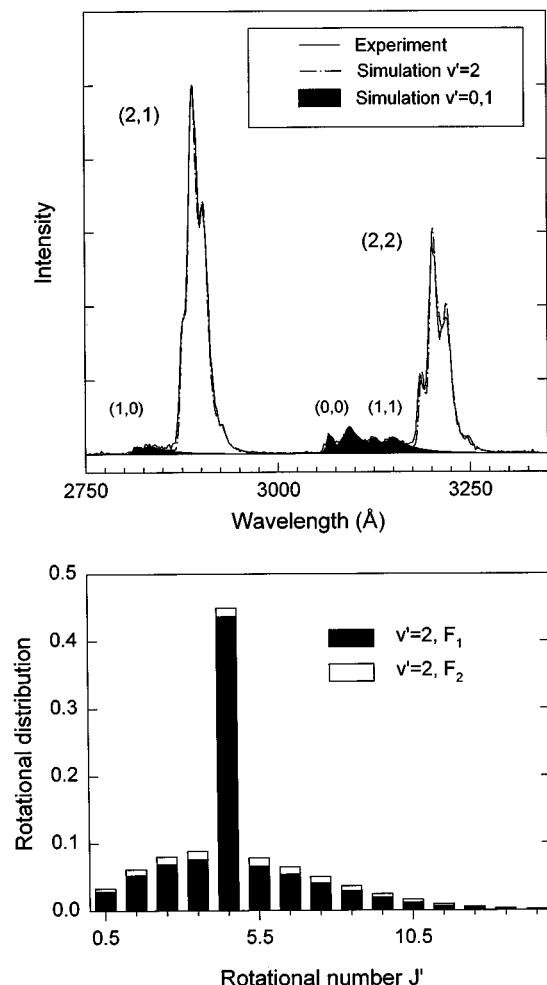


FIG. 3. Up: Fluorescence spectrum of OH (A-X) (2,1) and (2,2) after pumping  $Q_1(4)$  (2,0) in a  $\text{CH}_4\text{-O}_2$  flame at 7 Torr total pressure along with the simulated spectrum (8 Å FWHM). Down: Rotational distribution in OH A  $v'=2$  obtained from simulation of the above spectrum.

fluorescence is determined from a complete spectral simulation of the relevant vibrational bands, with tests against the high-resolution fluorescence scans to choose the proper rotational distributions. The simulation, computed with the program LIFBASE,<sup>15</sup> uses standard frequencies, line strengths, rotationally dependent predissociation, and radiative lifetimes, along with RKR wave functions and an optimized value<sup>13</sup> of  $R_e(r)$  following the *ab initio* form.<sup>4</sup>

### B. Vibrational level $v'=2$

A simulation of the (2,1) to (2,2) band region following excitation of  $v'=2$ , i.e., Fig. 3, was performed to determine the rotational population distribution in all three emitting vibrational levels. The rotational distribution within  $v'=2$  and the partitioning between the  $F_1$  and  $F_2$  spin components were varied until the simulated spectrum was judged to best match the experimental one. The fit is overlaid with the experimental spectrum and an inset shows the rotational distribution used. This distribution is dominated by the initially pumped level  $F_1(4)$  but shows that RET has occurred to

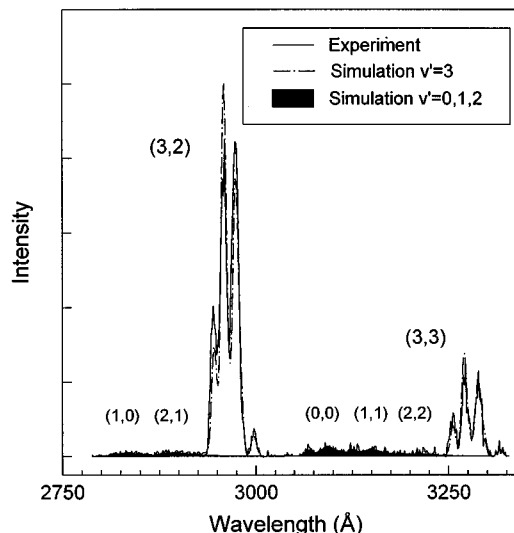


FIG. 4. Fluorescence spectrum of OH (A-X) (3,2) and (3,3) after pumping  $Q_1(4)$  (3,0) in a  $\text{CH}_4\text{-O}_2$  at 14 Torr total pressure along with simulated spectrum (8 Å FWHM), notice that the simulation does not take into account polarization of the fluorescence.

some extent. About 45% of the total  $v'=2$  population is found in  $N'=4$ , and the remaining 55% is distributed among other levels in a roughly 1000 K Boltzmann distribution; however, about 85% of the total population is retained within the  $F_1$  component even when RET has taken place. These results are in reasonable agreement with extrapolation of the rates of Lee *et al.*<sup>15</sup> who measured RET in  $v'=0$ , in collisions with  $\text{H}_2\text{O}$  in a  $\text{H}_2\text{-O}_2\text{-He}$  flame. Those rates predict that between one and two thirds of the population will undergo RET from  $N'=4$  during our 10 ns gate. Fluorescence from  $v'=0$  and 1, populated via VET, can be reasonably fit using a 2500 K Boltzmann distribution. These fits are also given in Fig. 3. It was found that 86% of the population remained in  $v'=2$  while 8% transferred to  $v'=1$  and 6% to  $v'=0$ . All these results are consistent with studies of VET from  $v'=1$  to 0 in a flame.<sup>16,17</sup>

Once the vibrational and rotational populations have been determined using the high resolution scans, the simulation is repeated with 3 and 4 nm resolution. The  $v'=0$  and 1 contributions to the experimental fluorescence spectrum are removed by subtracting the simulated spectrum. The amount of interference caused by VET in the total peak areas of the (2,1), (2,2), and (2,3) bands are 3%, 7%, and 4%, respectively.

Table I presents the  $p_{v'v''}$  from  $v'=2$  determined in this study, together with results from other investigations.

### C. Vibrational level $v'=3$

Simulations of the high resolution scan of the (3,2) and (3,3) band region are shown in Fig. 4, overlaid onto the experimental spectrum. In contrast to  $v'=2$ , there is a lack of rotational relaxation and very little VET into  $v'=0$ , 1, and 2. This is in accord with previous measurements following excitation of  $v'=3$  in low pressure flames.<sup>14</sup> All of the

TABLE I. Experimental relative emission coefficients for the vibrational levels  $v'=2$  to 3 along with the emission coefficients measured in other experiments. The experimental values are compared with the values obtained from simulation and previous calculations. The vibrational ratios have been normalized to (2,1) and (3,2) to facilitate the comparison.

Band	Experiment		Simulation		Calculations			
	This work	Refs. 5,11	$N'=4$	$v'=2, N'=2$ $v'=3, N'=11$	<i>Ab initio</i> Langhoff (Ref. 4)	<i>Ab initio</i> Popkie (Ref. 25 and 11)	Hyperbolic Chidsey (Ref. 26)	Linear Crosley (Ref. 11)
(2,0)	$250 \pm 30$	$230 \pm 25$	221	215	218	211	139	223
(2,1)	$1680 \pm 110$	$1790 \pm 100$	1525	1497	1535	1738	1780	1730
(2,2)	$1000 \pm 60$	1000	1000	1000	1000	1000	1000	1000
(2,3)	$11.5 \pm 0.8$	$12 \pm 2$	10.0	9.9	12.1	57	26	3.5
(2,4)	$6.0 \pm 0.5$	$6 \pm 3$	3.7	3.5	...	...	13	...
(2,5)	$0.7 \pm 0.2$		0.68	0.65	...	...	...	...
(3,0)	$21 \pm 2$	$19 \pm 4$	26	32	26.5	18	12	21
(3,1)	$312 \pm 30$	$260 \pm 30$	350	392	356	326	230	336
(3,2)	$1000 \pm 60$	1000	1000	1000	1000	1000	1000	1000
(3,3)	$265 \pm 30$	$280 \pm 40$	288	238	284	238	216	219
(3,4)	$3.0 \pm 0.6$	$3.3 \pm 0.8$	1.8	1.4	...	...	16	...
(3,5)	$9 \pm 1$	$6.4 \pm 1.4$	5.5	7.9	...	...	...	...
(3,6)	$\leq 1.5$	$\leq 2$	1.2	1.6	...	...	...	...

fluorescence emitted by  $v'=3$  can be attributed to the initially excited  $F_1(4)$  level. (It is noticeable that the experimental  $Q/P$  and  $Q/R$  branch ratios are smaller than in the simulation, owing to effects of polarization described below.) Simulations of bands with  $v'=0, 1$ , and 2, populated by VET, assume a 2500 K Boltzmann distribution. The vibrational population ratios were 99.55% in  $v'=3$ , 0.2% for  $v'=2$ , 0.15% for  $v'=1$ , and 0.1% in  $v'=0$ . However, because these lower levels have a higher quantum yield than does  $v'=3$ , they contribute a proportionately larger fraction of the total emission.<sup>13</sup> The bands populated by VET contribute 1%, 3%, and 4%, respectively, to the observed areas of (3,2), (3,3), and (3,4).

The differences between the spectra when initially exciting  $v'=2$  and 3 can be explained by the difference in predissociative lifetime. These are about 100 ns<sup>20</sup> for low-lying rotational levels of  $v'=2$  but only 0.25 ns<sup>21,22</sup> for low  $N'$  in  $v'=3$ . Thus in  $v'=2$  there is ample time for RET and depolarization collisions to occur, whereas  $v'=3$  predissociates before collisional processes occur to any significant extent in our low pressure flame.

## D. Polarization of $v'=3$ fluorescence

The polarization of the fluorescence from  $v'=3$  can cause problems in the determination of the band ratios. This is because there is a difference in reflectance by the monochromator grating for light polarized parallel or perpendicular to its grooves, and this difference has a wavelength dependence. The spectral response calibration, on the other hand, was performed with unpolarized light.

The polarization of LIF from OH in flames has been investigated previously,<sup>23</sup> including the derivation of expressions for the degree of polarization expected under collision-free conditions as pertinent to  $v'=3$ . Information relevant to the present study is given in Table II, which lists for Q-branch excitation the relative intensities of each rotational

branch in fluorescence, polarized parallel and perpendicular to the direction of polarization of the exciting radiation. As can be seen, these differ depending on whether  $Q$ ,  $R$ , or  $P$  is being observed. To obtain the total intensity polarized in a given direction, one must multiply the polarization values of Table II by the appropriate Einstein emission coefficients. That is,  $I_{\perp} = A_Q I_{\perp Q} + A_P I_{\perp P} + A_R I_{\perp R}$  and similarly for  $I_{\parallel}$ . For example, consider the high  $J$  limit, where  $I_Q = 2I_R = 2I_P$ . Then, for vertical laser polarization, the intensity polarized vertically ( $I_{\parallel}$ ) is 1.33 times the light polarized horizontally ( $I_{\perp}$ ). The next step in the calculation requires knowledge of the geometry of the experiment. In our case, observation is in a direction perpendicular to the laser beam propagation direction. For the low resolution experiments, the laser was polarized vertically, that is, perpendicular to the plane formed by the laser beam and observation direction. In this case, the relevant quantity is  $I_{\perp} + I_{\parallel}$ . For the higher resolution scans the laser was polarized horizontally, in the plane, so the quantity of interest would be  $2I_{\perp}$ .

To evaluate the wavelength dependence of the influence of polarization, we use typical grating response curves furnished by the monochromator manufacturer. Most data of interest were obtained using the 500 nm blaze grating, at wavelengths below 500 nm. The grating efficiencies are

TABLE II. Intensity  $I_{\parallel}$  and  $I_{\perp}$  to the laser polarization. Excitation in the  $Q$  branch is assumed.

Observed branch	$I_{\parallel}$	$I_{\perp}$	$I_{\parallel}(J'=4.5)$	$I_{\perp}(J'=4.5)$
$Q$	$\frac{3J^2+3J-1}{J(J+1)}$	$\frac{2J^2+2J+1}{2J(J+1)}$	2.96	1.02
$R$	$\frac{J-1}{J}$	$\frac{4J+1}{2J}$	0.78	2.11
$P$	$\frac{J+2}{J+1}$	$\frac{4J+3}{2(J+1)}$	1.18	1.91

equal at 500 nm, i.e., the same as for unpolarized light, but at 250 nm  $I_{\parallel}$  is collected 2.85 times more efficiently than  $I_{\perp}$ . Using the values of Table II for the actual  $J=4.5$ , and the appropriate Einstein coefficients, one can calculate that, for vertical laser polarization, the total (polarized) fluorescence at 250 nm is detected with 7% lower efficiency than unpolarized light. A similar analysis for the 250 nm grating yields a maximum error of 2%.

Assuming a linear interpolation of correction vs wavelength, the intensities of the weak (3,0) and (3,4) bands, relative to the strong (3,2) band, are detected with a maximum error due to polarization of  $-1.4\%$  and  $-1.9\%$ , respectively. The error in the stronger (3,1) and (3,2) bands are  $-0.8\%$  and  $+0.9\%$ . This is much less than experimental error and has not been applied to the values listed in Table I.

### E. The (2,2)/(2,1) ratio

The first LIF study of transition probabilities in OH, by CL,<sup>11</sup> yielded a ratio of experimental intensities for the important (1,1) and (1,0) bands of  $1.58 \pm 0.16$  ( $2\text{-}\sigma$  error). This was just outside agreement with the value 1.75 predicted by a linear  $R_e(r)$  fitted by CL to seven band ratios including this value of  $p_{1,1}/p_{1,0}$  itself. (The most recent theoretical treatment<sup>13</sup> using the *ab initio* moment predicts the same value as the linear moment.) This troubling disagreement led to a careful consideration of potential systematic error but none was found. The subsequent LIF determination by Copeland *et al.*<sup>12</sup> produced a ratio  $1.64 \pm 0.15$ , within  $2\text{-}\sigma$  error of the predicted value but still lower.

From the current study, we scrutinize the (2,2) and (2,1) bands, having an  $r$ -centroid difference similar to that of the (1,1) and (1,0) bands. The (2,2)/(2,1) ratio of  $0.60 \pm 0.08$  ( $2\text{-}\sigma$ ) determined in the high-resolution scans is 7% higher than that determined in the low-resolution scans (0.56). Because the vibrational levels populated by VET are more accurately fit in the high-resolution scan, we tend to prefer that value. On the other hand, CL's experimental value is  $0.56 \pm 0.04$ . As for the case of 1,1 and 1,0, the experimental results from CL and the current low resolution scans are smaller than the optimized theoretical prediction<sup>13</sup> of 0.64. Attempting to clarify this issue, we made a brief series of measurements of the  $p_{2,2}/p_{2,1}$  ratio in a low pressure cell, where the OH was produced via  $\text{HNO}_3$  photolysis. These experiments, described in more detail in Ref. 19, were not entirely conclusive, due to some concerns about calibration of the optical system. However, they tend to support the slightly higher value. Thus the experimental and theoretical values for  $p_{2,2}/p_{2,1}$  appear in agreement even though the residual discrepancy for the well studied  $p_{1,1}/p_{1,0}$  ratio is not understood.

### F. Experimental uncertainties

The experimental uncertainties in this work are of two kinds: A statistical error computed from replicate measurements of each band, and a systematic error from the monochromator/detector response calibration. As discussed below, the former dominates our results, and constitutes the

$2\text{-}\sigma$  errors quoted in Table I. These come from a minimum of six measurements for each ratio, in some cases more.

As noted above, two different spectral lamps are used to calibrate the relative spectral response as a function of wavelength. The tungsten standard lamp has an output flux at 500 nm that is nearly a thousand times that at 250 nm. While possible in principle to use this one lamp throughout the entire spectral region, this large flux difference poses practical problems. Stray visible light in the monochromator poses troublesome background at the shortest wavelengths. Therefore the deuterium lamp provides the calibration source between 200 and 350 nm. We overlap the calibrated response between 300 and 350 nm using both lamps, to obtain total response over the entire range of interest.

From considerations of the noise in the lamps, and uncertainty in the relative output of each lamp as a function of wavelength from manufacturer estimates, the calibration error is less than 5% over the entire range 200–500 nm. However most of the bands important for determining the transition moment<sup>13</sup> span a smaller wavelength range, the error is accordingly less, on the order of 2% at most. This error is considerably smaller than the statistical uncertainty and is not included in the total uncertainty quoted in Table I.

## IV. DISCUSSION

Table I compiles results from the present work and selected previous experimental values and theoretical calculations. The experimental comparisons for this work are LIF studies by CL<sup>11</sup> for the  $v'=2$  level and AM<sup>5</sup> for  $v'=3$ . Agreement is excellent between this study and that of Ref. 11. CL excited  $N'=2$  in a flow cell at 10–20 mTorr where RET is negligible, so that reported ratios are for emission solely from that level. In our experiment, over 50% of the population has shifted from  $N'=4$  toward a Boltzmann distribution near 1000 K. Calculated relative emission intensities for this partially relaxed population distribution differ by less than 1% from that for  $N'=4$  alone. In turn, calculated values of relative band emission intensities for  $N'=2$  and  $N'=4$ , listed in Table I, differ by less than 5%, showing that we may compare our results directly with those of CL for  $N'=2$ ; all differences are within error bars. In addition, we have extended these measurements to the (2,5) band.

We compare our  $v'=3$  relative emission intensities for  $N'=4$  with those of AM,<sup>5</sup> who excited  $N'=11$  with a KrF excimer laser in an atmospheric pressure flame. The high-resolution fluorescence spectrum exhibited in Ref. 5 shows that no RET occurs in that experiment, so that the results should be specific to the  $N'=11$  level. Calculations comparing relative band transition probabilities for  $N'=4$  and 11 are given in Table I. These predict a strong rotational level dependence, with differences as much as 25% for strong bands. Curiously, the experimental results of AM are much closer to our  $N'=4$  values than would be foreseen from the calculated rotational dependence, overlapping within  $1\text{-}\sigma$  errors in all cases. The reason for this unexpected level of agreement is not known. A future systematic study of the

dependence of the  $v'=3$  vibrational transition probabilities with rotational level may clarify this issue.

Also included in Table I are transition probabilities calculated using selected forms of  $R_e(r)$  and the vibrational wave functions in each state. An empirical linear form, first suggested by Shuler,<sup>24</sup> was optimized by CL using Morse oscillators. This describes well the strong bands  $v'=2$ ,  $v''=0-2$ , and  $v'=3$ ,  $v''=0-3$ . The first *ab initio*  $R_e(r)$ , by Henneker and Popkie,<sup>25</sup> was linear over the range of internuclear distance they considered; this calculation of  $p_{v',v''}$  used RKR wave functions. This early attempt was as good as the empirical linear  $R_e(r)$ , but the most recent *ab initio* form, by Bauschlicher and Langhoff,<sup>4</sup> is much better. This  $R_e(r)$  falls within uncertainty limits of a moment fitted<sup>13</sup> to empirical data (including the present results) using RKR wave functions.

In conclusion, we have measured relative emission intensities for the  $v'=2$ , and  $v'=3$ ,  $v''$  sequences of the  $A^2\Sigma^+ - X^2\Pi_i$  transition of the OH radical. Our results are in generally good agreement with previous experiments on these levels, and add a determination of the (2,5) band. The bands measured here involve vibrational wave functions spanning a wide range of internuclear distance, making them useful for an overall empirical optimization of  $R_e(r)$  for this electronic band system.<sup>13</sup> The (3,1) and (2,1) bands show somewhat better agreement with theoretical calculations than previous work.

## ACKNOWLEDGMENTS

This research was supported by the Basic Research Group of the Gas Research Institute and the National Aeronautics and Space Administration's Global Tropospheric Program. During part of this study, J. Luque was an SRI International Fellow sponsored by the Ministerio de Educacion y Ciencia, Spain. K. L. Steffens was also with the Department of Chemistry, Stanford University.

- <sup>1</sup>D. E. Heard, J. B. Jeffries, G. P. Smith, and D. R. Crosley, *Comb. Flame* **88**, 137 (1992).
- <sup>2</sup>D. R. Crosley, *J. Atmos. Sci.* **52**, 3297 (1995).
- <sup>3</sup>K. G. McKendrick, D. J. Rakestraw, R. Zhang, and R. N. Zare, *J. Phys. Chem.* **92**, 5530 (1988).
- <sup>4</sup>C. W. Bauschlicher and S. R. Langhoff, *J. Chem. Phys.* **87**, 4665 (1987).
- <sup>5</sup>P. Andresen, A. Bath, W. Gröger, H. W. Lülff, G. Meijer, and J. J. ter Meulen, *Appl. Opt.* **27**, 365 (1988).
- <sup>6</sup>G. P. Smith and D. R. Crosley, *J. Geophys. Res.* **95**, 16427 (1990).
- <sup>7</sup>K. J. Rensberger, J. B. Jeffries, and D. R. Crosley, *J. Chem. Phys.* **90**, 2174 (1989).
- <sup>8</sup>I. J. Wysong, J. B. Jeffries, and D. R. Crosley, *J. Chem. Phys.* **94**, 7547 (1991).
- <sup>9</sup>C. H. Dieke and H. M. Crosswhite, *J. Quant. Spectrosc. Radiat. Transfer* **2**, 97 (1962).
- <sup>10</sup>P. E. Rouse and R. J. Engleman, *J. Quant. Spectrosc. Radiat. Transfer* **13**, 1503 (1973).
- <sup>11</sup>D. R. Crosley and R. K. Lengel, *J. Quant. Spectrosc. Radiat. Transfer* **15**, 579 (1975).
- <sup>12</sup>R. A. Copeland, J. B. Jeffries, and D. R. Crosley, *Chem. Phys. Lett.* **138**, 425 (1987).
- <sup>13</sup>J. Luque and D. R. Crosley, *J. Chem. Phys.* (to be published).
- <sup>14</sup>K. L. Steffens, J. B. Jeffries, and D. R. Crosley, *Opt. Lett.* **18**, 1355 (1993).
- <sup>15</sup>J. Luque and D. R. Crosley, "LIFBASE: Database and Spectral Simulation Program," SRI International Report MP 96-001, 1996.
- <sup>16</sup>M. P. Lee, R. Kienle, and K. Kohse-Hoinghaus, *Appl. Phys. B* **58**, 447 (1994).
- <sup>17</sup>G. P. Smith and D. R. Crosley, *Appl. Opt.* **22**, 1428 (1983).
- <sup>18</sup>A. T. Hartlieb, D. Markus, W. Kreutner, and K. Kohse-Hoinghaus, *Appl. Phys. B*, (submitted).
- <sup>19</sup>K. L. Steffens, Ph.D. thesis, Stanford University (1994).
- <sup>20</sup>J. Brzozowski, P. Erman, and M. Lyrre, *Phys. Scripta* **17**, 507 (1978).
- <sup>21</sup>J. A. Gray and R. L. Farrow, *J. Chem. Phys.* **95**, 7054 (1991).
- <sup>22</sup>D. E. Heard, D. R. Crosley, J. B. Jeffries, G. P. Smith, and A. Hirano, *J. Chem. Phys.* **96**, 4366 (1992).
- <sup>23</sup>P. M. Doherty and D. R. Crosley, *Appl. Opt.* **23**, 713 (1984).
- <sup>24</sup>K. E. Shuler, *J. Chem. Phys.* **18**, 1221 (1950).
- <sup>25</sup>W. H. Henneker and H. E. Popkie, *J. Chem. Phys.* **54**, 1763 (1971).
- <sup>26</sup>I. L. Chibsey, D. R. Crosley, *J. Quant. Spectrosc. Radiat. Trans.* **23**, 187 (1980).